

STUDY OF EP INSTABILITY FOR A COASTING PROTON BEAM IN CIRCULAR ACCELERATORS

K. Ohmi, T. Toyama, M. Tomizawa
 KEK, 1-1 Oho, Tsukuba, 305-0801, Japan

Abstract

We discuss interactions between a coasting proton beam and electrons. The electrons, which are created near the beam position, are considered in this paper. A coasting proton beam traps the electrons eternally, if there is not perturbations nor diffusion mechanisms. Therefore electrons are accumulated and their density could arrive above a threshold value for the instability, finally: i.e., a coasting proton beam is always unstable. However the instability affects both of the beam and electrons. Electrons may be diffused by the instability, in which the beam still has a small oscillation amplitudes, with the result that the beam amplitude may be kept in the small level, and may be stable in actual operations of accelerators. We study the ep instability with focusing the electron diffusion using a computer simulation method.

INTRODUCTION

We study ep instability for a coasting beam, in which the charged distribution is uniform along the longitudinal axis z . A static electric potential is formed by the coasting beam, when there is no transverse motion. Electrons created near the beam are trapped eternally, while electrons created at the chamber wall are absorbed with the same energy as those at the creation. Proton beam, which ionizes residual gas, creates electrons near the beam. The electrons, which are trapped, are accumulated, and their density arrives a threshold of the ep instability. Above the threshold, both of the beam and electron cloud become unstable. To be precise, amplitude of electrons is much larger than that of the beam, as is shown in later. The beam-electron force is strongly nonlinear. The electrons with a large amplitudes due to the instability are smeared by the nonlinear force. The size of the electron cloud is enlarged, and electrons are absorbed into the chamber wall.

Electrons are also created at the chamber wall due to proton beam loss and secondary electron. The energy of the electrons is the order of 10 eV, except some portion with an energy equal to incident one. Therefore the multipacting does not develop naively in the coasting beam, because the initial energies of electrons are kept at their absorption. The beam with a perturbation traps the electrons created at the chamber during a short period or accelerates them to higher energy than initial one. Therefore the multipacting may be important even in the coasting beam. This is the same physics in the meaning of the transition between the trapping and diffusion.

We focus the ionization electrons and their diffusion in

this paper, and will discuss somewhere the extension to surface electrons and multipacting for the coasting beam.

Ionization cross-section for CO and H₂ is estimated to be $\sigma(\text{CO}) = 1.3 \times 10^{-22} \text{ m}^2$ and $\sigma(\text{H}_2) = 0.3 \times 10^{-22} \text{ m}^2$ using the Bethe formula [1]. The molecular density d_m is related to the partial pressure in nPa using the relation at 20°C, $d_m(\text{m}^{-3}) = 2.4 \times 10^{11} P_m(\text{nPa})$. The electron production rate is $7.7 \times 10^{-9} e^- / (\text{m}\cdot\text{p})$ at $2 \times 10^{-7} \text{ Pa}$.

The instability is characterized by the frequency of electron in the potential of the coasting beam,

$$\omega_e = \sqrt{\frac{\lambda_p r_e c^2}{2\sigma_{x(y)}(\sigma_x + \sigma_y)}}. \quad (1)$$

Landau damping, which is caused by the longitudinal slippage, is conjectured to be very strong, since the frequency is very rapid, $n \equiv \omega_e/\omega_0 \gg 1$.

Linear theory is reviewed in Sec.2, and beam stability and the electron diffusion using a particle tracking method is discussed in Sec.3.

LINEAR THEORY AND THRESHOLD OF THE INSTABILITY

We survey linear theory of ep instability [2], and estimate the threshold at some high intensity proton rings in the world. The interactions between the beam and electron cloud is represented by a wake force [3]. The wake force is expressed by

$$W_1(z) = c \frac{R_S}{Q} \frac{\omega_e}{\tilde{\omega}} \exp\left(\frac{\alpha}{c} z\right) \sin\left(\frac{\tilde{\omega}}{c} z\right), \quad (2)$$

where

$$cR_S/Q = \frac{\lambda_e}{\lambda_p} \frac{L}{(\sigma_x + \sigma_y)\sigma_y} \frac{\omega_e}{c}. \quad (3)$$

in the language of impedance, we would say that the Q factor is infinite. Actually the frequency spread of ω_e should be taken into account. By taking into the frequency spread of ions, $\Delta\omega_e = \omega_e/2Q$, the impedance is given by

$$Z_1(\omega) = \frac{c}{\omega} \frac{R_S}{1 + iQ \left(\frac{\omega_e}{\omega} - \frac{\omega}{\omega_e} \right)} \quad (4)$$

$$= \frac{\lambda_e}{\lambda_p} \frac{L}{\sigma_y(\sigma_x + \sigma_y)} \frac{\omega_e Z_0}{\omega 4\pi} \frac{Q}{1 + iQ \left(\frac{\omega_e}{\omega} - \frac{\omega}{\omega_e} \right)},$$

where Z_0 is the vacuum impedance 377Ω.

We discuss the stability of a beam which experiences the effective impedance. The stability criterion for the coasting beam is given by the dispersion relation as follows [4],

$$U \equiv \frac{\sqrt{3}\lambda_p r_p \beta \omega_0}{\gamma \omega_e \eta \sigma_{\delta E/E}} \frac{|Z_1(\omega_e)|}{Z_0}, \quad (5)$$

where β is a typical value of the beta function in a ring, and r_p is the classical proton radius. This formula is the same as that given by Keil and Zotter for e-p instability [2]. For $U > 1$, the beam is unstable. The thresholds of the neutralization factor are given by

$$f_{th} = \frac{2\pi\gamma n \eta \sigma_{\delta}}{\sqrt{3}\lambda_p r_p \beta Q} \frac{\sigma_{x(y)}(\sigma_x + \sigma_y)}{L} \quad (6)$$

We put 5 and 10 m for Q and β , respectively, and the threshold values for various rings are shown in Table 1.

SIMULATION USING BEAM TRACKING

Before going to beam tracking we study electron motion trapped in the beam potential. Fig. 1 shows samples of electron trajectories for (a) static beam potential and for (b) including a perturbation due to a coherent motion of beam. Motion of three samples of electrons are depicted in Fig. 1(a). It shows that electrons are trapped in the potential. Fig. 1(b) depicts motion of an electron in a perturbed potential. The amplitude of the electron gradually increase as time goes by.

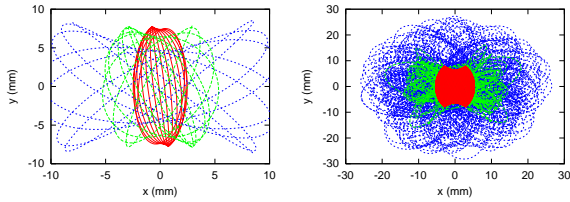


Figure 1: Trajectory of electrons. (a) Three electrons are tracked without perturbation. (b) An electrons are tracked with perturbation. Green and blue points are phase space coordinate of electron during 10 turns and 100 turns, respectively. Red points are those without perturbation as a reference.

We study the motion of proton beam interacting with the electron cloud using a tracking simulation.

A coasting proton beam is represented by macro-particles which are located along z with equal spacing. Each macro-particle has a charge and a mass corresponding to the proton line density. The macro-particle (proton) can undergo dipole motion with a dipole moment characterized by $\bar{x}_{p,i}(z_i, s) = (\bar{x}_p, \bar{y}_p)$, but the emittance (size) is kept constant. The number of macro-protons should be more $\omega_e L/c$, because electrons in the cloud oscillate smoothly by the force from the macro-protons. The electron cloud is created at some positions in the ring, and is represented by a

large number of point-like macro-particles denoted by $x_{e,a}$ ($a = 1, N_e$). The electrons are created in every passage of the proton beam. The transverse position of electrons is randomly generated with the same rms size as the beam.

The motion of the macro-electrons and macro-protons is tracked during the beam passage. After that, macro-protons are transported by the lattice magnets. This procedure is repeated in every interaction of the bunch with the cloud. Electrons are absorbed at the chamber wall surface. The number of macro-electrons increases except their disappear at the wall.

We take into account the Landau damping caused by the longitudinal motion, which disturbs the coherence of the dipole motion. The Landau damping rate per one revolution is given by $\alpha = n\eta\sigma_{\delta E/E}/\sqrt{3}$ for the coasting beam, where $n = \omega_e/\omega_0$. In the simulation, the Landau damping is treated by a simple way as

$$\bar{x}_{p,i} = (1 - \alpha)\bar{x}_{p,i}. \quad (7)$$

We performed the simulation for J-PARC 50 GeV rings at the flat top. The damping rate is 1.1×10^{-3} . The threshold line density is $\lambda_e = 4.5 \times 10^8 \text{ m}^{-1}$. Electron production rate per one revolution time T_0 is $7.7 \times 10^{-9} e^- / (\text{m}\cdot\text{p}) \times 21.2 \times 10^{10} \times 1567 = 2.5 \times 10^6 \text{ m}^{-1} T_0^{-1}$ for $P = 2 \times 10^{-7} \text{ Pa}$. The production rate linearly depends on the vacuum pressure. The build up time up to the threshold is 180 turns (0.9 ms) in linear theory. We put 10 interaction points in the ring. The dipole motion is assumed to be periodic for the 1/10 divided part of the whole ring: that is, the beam (macro-proton train) with 1/10 length is tracked. The beam (1/10 part) is represented by 1000 macro-protons. $\omega_e L/10c = 774$ is $\gg 1$ and < 1000 .

The simulations were performed for several electron production rates. Amplitudes of each macro-proton ($J_{x(y),i}$), electron line density (λ_e), electron rms. size (σ_e), etc. were obtained by the simulation. There was no significant result for the production rate of $2.6 \times 10^5 \text{ m}^{-1} T_0^{-1}$, correspond to $P = 2 \times 10^{-7} \text{ Pa}$. Fig. 2 shows λ_e , maximum amplitude of $\sqrt{J_{x(y)}}$ and σ_e for the electron production rate, $2.6 \times 10^6 \text{ m}^{-1}$ ($P = 2 \times 10^{-6} \text{ Pa}$). All of them increase and is saturated at 3000 turn. The saturation of the beam amplitude is $\sigma_r/100$. We may not observe the instability due to the small amplitude.

Fig. 3 shows electron line density λ_e and maximum amplitude $\sqrt{J_{x(y)}}$ for various electron production rates of $2.6 \times 10^7 \text{ m}^{-1} T_0^{-1}$, $2.6 \times 10^8 \text{ m}^{-1} T_0^{-1}$ and $2.6 \times 10^9 \text{ m}^{-1} T_0^{-1}$. Converting to the vacuum pressure, the rates are $P = 2 \times 10^{-5} \text{ Pa}$, $2 \times 10^{-4} \text{ Pa}$ and $2 \times 10^{-3} \text{ Pa}$, respectively. The saturation levels are $\sigma_r/30$, $\sigma_r/10$ and σ_r , respectively. If we can observe the instabilities with a resolution of 10% of σ_r , the production rate should be more than $10^8 \text{ m}^{-1} T_0^{-1}$, which corresponds to 10^{-4} Pa . This value is too high for the vacuum pressure.

Table 1: Basic parameters and threshold of the neutralization factor of the proton rings

variable	symbol	JPARC-MR	KEK-PS	PSR	ISIS	AGS-Bst.	AGS	FNAL-MI
circumference	L (m)	1567.5	339	90	163	202	800	3319
relativistic factor	γ	54.	12.8	1.85	1.07	1.2	3.0	128
beam line density	$\lambda_p (\times 10^{10}) \text{ m}^{-1}$	21.2	0.74	33.3	18.4	82.7	8.75	0.90
rms beam sizes	σ_r (cm)	0.35	0.5	1.0	3.8	1	0.7	0.17
rms energy spread	$\sigma_{\delta E/E}$ (%)	0.25	0.3	0.4	0.5	0.5	0.28	0.03
transition energy	γ_t	31.6 <i>i</i>	6.76	3.08	5.07	4.88	8.5	21.8
slippage factor	η	-0.0013	0.016	-0.187	-0.83	-0.652	0.0122	0.0020
	$\omega_e L/c$	7740	225	195	69	226	2012	6930
Threshold	f_{th} (%)	0.21	4.0	2.5	45.	15.	2.6	0.06

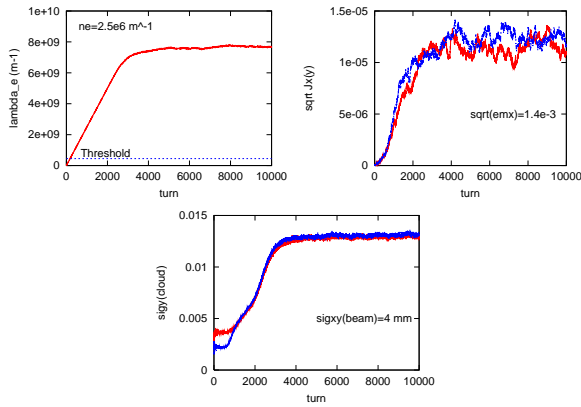


Figure 2: Evolution of line density of electron cloud (λ_e [m^{-1}]), maximum amplitude of beam ($J_{x(y)}^{1/2}$ [$\text{m}^{1/2}$]) and size of electron cloud ($\sigma_{x(y)}$ [m]) for the electron production rate of $2.6 \times 10^6 \text{ m}^{-1} T_0^{-1}$.

CONCLUSION

We have studied ep instability for a coasting proton beam. Electrons created by ionization are treated in this paper. The instability is not caused by electron cloud for slow production rate. Production rate is important whether the instability grow to visible amplitudes. The production rate more than $10^8 \text{ m}^{-1} T_0^{-1}$ is required to be unstable for JPARC-MR ring. The rate corresponds to 10^{-4} Pa , which is quite nonsense. Ionization may not be a direct candidate of the instability. Electron sources with a higher production rate, for example, proton loss and/or multipacting have an essential role even for the coasting beam instability.

Similar analysis and discussion can be extended to the beam-ion instability in electron storage rings straightforwardly.

The authors thank the members of the electron-proton instability working group of J-PARC, N. Hayashi, S. Kato, K. Satoh, S. Machida, K. Oide K. Yokoya for fruitful discussions.

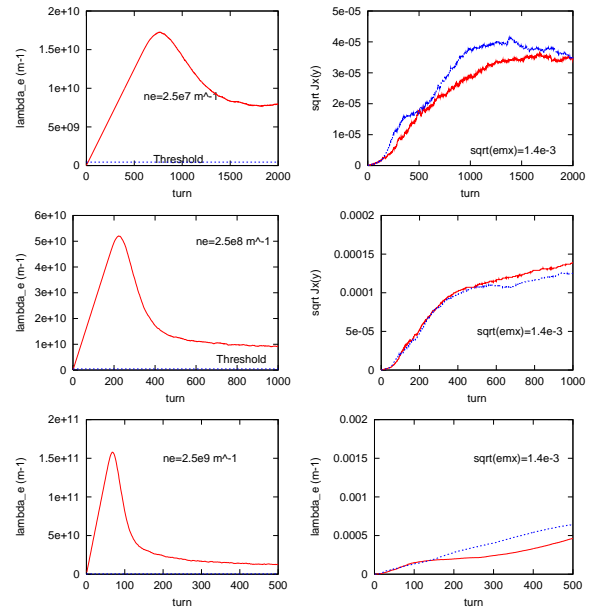


Figure 3: Evolution of line density of electron cloud (λ_e [m^{-1}]) and maximum amplitude of beam ($J_{x(y)}^{1/2}$ [$\text{m}^{1/2}$]) for the electron production rates of $2.6 \times 10^7 \text{ m}^{-1} T_0^{-1}$, $2.6 \times 10^8 \text{ m}^{-1} T_0^{-1}$ and $2.6 \times 10^9 \text{ m}^{-1} T_0^{-1}$.

REFERENCES

- [1] Y. Baconnier, CERN report 85-19, pp.267 (1985).
- [2] E. Keil and B. Zotter, CERN-ISR-TH/71-58 (1971).
- [3] K. Ohmi, T. Toyama, C. Ohmori, Phys. Rev. ST-AB.,5, 124402 (2002).
- [4] E. Keil and W. Schnell, CERN Report TH-RF/69-48 (1969).